Condensation rate-mass flux correlation: implications for supersaturation in shallow cumulus clouds

Yefim L. Kogan

NorthWest Research Associates, Inc. Redmond, WA 98052-5164

Phone: 858-365-7922 email: ykogan@nwra.com

MOTIVATION

In our previous study (Kogan 2021) we found that a remarkably strong correlation exists between integral cloud condensation rate and integral upward mass flux. The current investigation provides the physical basis for such relationship and implication for evaluating supersaturation in convective clouds.

APPROACH

The research is based on the LES simulations initialized with observations from Rain In Cumulus over the Ocean (RICO) field project. They provide dynamically balanced 3D datasets necessary for obtaining statistically robust dependencies between variables. The analysis is facilitated by stratifying clouds by cloud top and cloud maturity.

MODEL SETUP

Our LES model (SAMBM) employs the dynamical core of the System for Atmospheric Modeling (SAM, Khairoutdinov and Randall 2003) and the Bulk Microphysics (BM, Kogan 2013) fine-tuned for shallow Cu convection. The observations from the RICO field campaign (van Zanten et al 2011) were used for initialization of the LES simulations conducted in a rather large 50.0×50.0×4 km^3 domain (500×500×100 grid points).

DATASET

Over the course of the simulation from 8 to 32 hours, we selected 2031 clouds that were collected every 30 minutes. In order to facilitate the analysis of the complex system of clouds at various stages of their development, the dataset was sorted out by cloud top height and divided into four groups G1-G4, each of which condenses approximately equal amount of water vapor

per second. The groups G1-G2 represent clouds mostly in the growing stage, while groups G3-G4, on the contrary, contain mature and decaying clouds.

CONDENSATION RATE – MASS FLUX RELATIONSHIP

In our previous study (Kogan 2021) we found that a remarkably strong correlation exists between the integral cloud condensation rate and the integral mass flux (see Fig. 1).

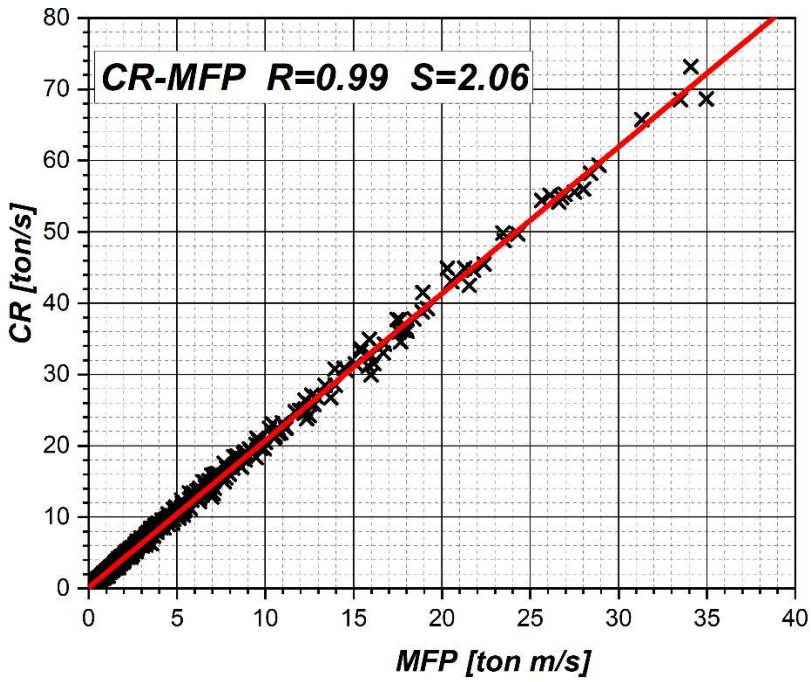

Fig 1. Scatter plots of condensation rates (CR) as a function of upward mass flux (MFP) for clouds in all groups. R is the correlation coefficient; S is the slope of the linear fit.

The functional relationship between the condensation rate ($\frac{dq_l}{dt}$) and upward mass flux ($\rho_a W$) can be expressed as a linear function:

$$\frac{dq_l}{dt} = \alpha_{les}\rho_a W \tag{1}$$

where α_{les} = 2.06 x10^{-6} [s^{-1}]. Here liquid water content q_l and air density ρ_a are in kg m^{-3}, vertical velocity W in ms^{-1}. The coefficients α_{les} for individual cloud groups slightly differ from

the coefficient for the whole dataset (Fig. 2). They are 4-5% higher for small growing clouds (2.17 for G1 and 2.13 for G2), while lower for larger clouds (2.052 for G3 and 2.049 for G4 clouds).

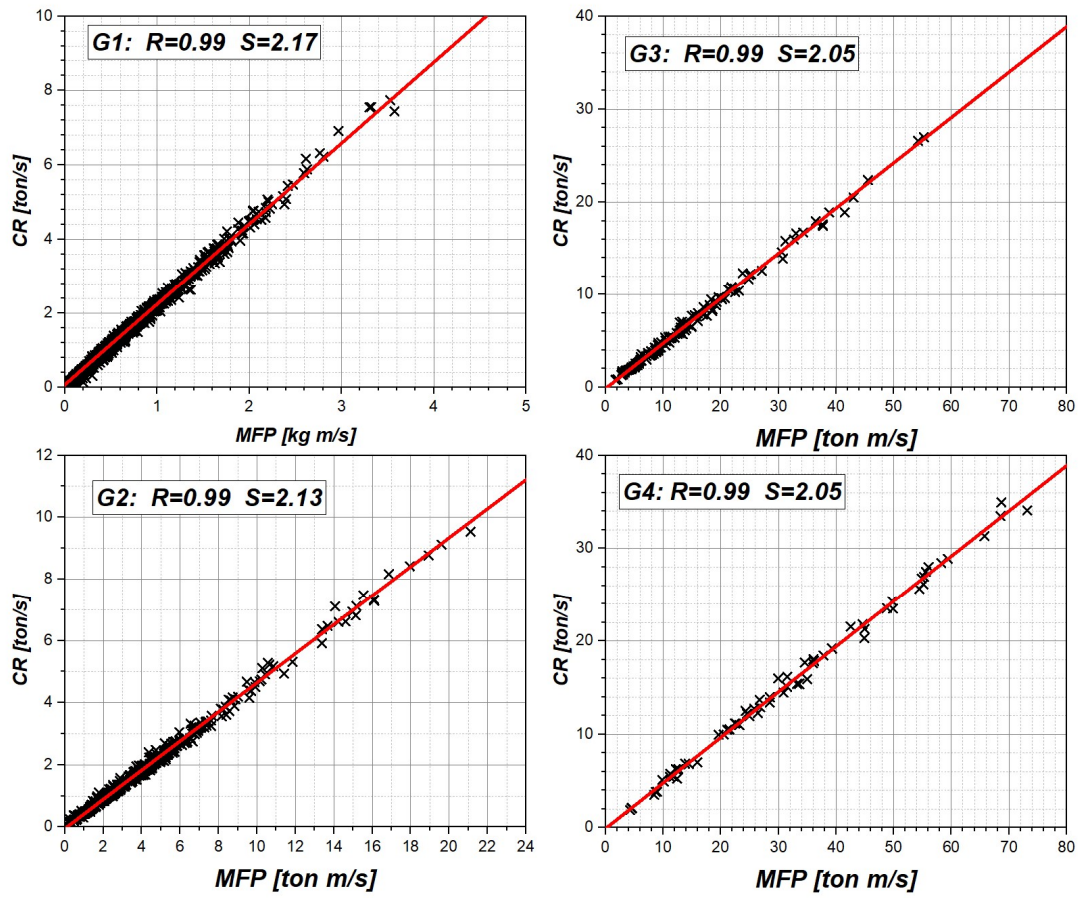

Fig. 2. Scatter plots of condensation rates (*CR*) as a function of upward mass flux (*MFP*) for clouds in each of the four groups. *R* is the correlation coefficient; *S* is the slope of the linear fit.

The subscript *'les'* denotes that coefficient α_{les} in (1) is obtained from LES model data, as opposite to theoretical formulation described in the next section.

Obviously, using the specific latent heat constant, one can directly relate formulation (1) to the latent heat produced during phase transitions.

THEORETICAL FORMULATION OF THE *CR –MFP* RELATIONSHIP

The SAMBM model used in our study is a so-called two and half moment model, i.e., it employs three prognostic moments for cloud water variables (q_c, n_c and R_i) and two moments for rain water variables (q_r, n_r) (Khairoutdinov and Kogan, 1999). The use of an additional cloud moment, the integral radius $R_i = \int rn(r)dr$ ($n(r)$ is the drop size distribution function), is essential as it allows direct calculation of phase transition rates. Specifically, using the condensational growth equation for the cloud drop with radius r

$$\frac{dr}{dt} = \frac{G(T,P)S}{r} \tag{2}$$

and having R_i as a prognostic variable in the model, we can calculate the rate of change of cloud liquid water content:

$$\frac{dq_l}{dt} = 4\pi\rho_w G(T,P)SR_i \tag{3}$$

Here S and R_i are supersaturation and integral cloud drop radius, ρ_w and ρ_a are water and air density, respectively. The coefficient $G(T,p)$ is a weak function of temperature T and pressure P.

For numerical solution of equation (3), we first calculate at each time step the changes in temperature and water vapor due to advection and turbulent mixing. The corresponding intermediate values of T^* and Q_v^* are used to calculate supersaturation S, and, based on it, condensation/evaporation rates according to (3). This splitting of dynamical and microphysical terms is analogous to a 1D Lagrangian air parcel model where the two terms in the supersaturation equation account for dynamical ascent/descent, as well as latent heat release (e.g., Squires 1952, Paluch and Knight 1984).

$$\frac{dS}{dt} = A_1W - A_2SR_i \tag{4}$$

In (4) coefficients A_1 and A_2 are weak functions of temperature T and pressure P (Politovich and Cooper, 1988, Pinsky et al 2013). As was shown in many studies of supersaturation in clouds (e.g., Paluch and Knight, 1984, Cooper 1989, Korolev and Mazin 2003, Pinsky et al

2013, Siebert and Shaw 2017), for times larger than phase relaxation time, the equation (4) has an asymptotic "quasi-steady" solution for S:

$$S_{qs} = \frac{A_1 W}{A_2 R_i} \tag{5}$$

The quasi-steady supersaturation is an important characteristic of the condensation process, as it corresponds to an equilibrium between contributions to the supersaturation equation (4) from dynamical and microphysical processes. It is convenient, therefore, to measure the actual cloud supersaturation in units of S_{qs}:

$$S = \kappa S_{qs} \tag{6}$$

Substituting (6) into (3) and using expression (5), we can rewrite (3) as:

$$\frac{dq_l}{dt} = \frac{4\pi\rho_w G A_1}{A_2}\kappa W = \kappa\frac{A_1}{A_3}\rho_a W = \kappa\alpha_{qs}\,\rho_a W \tag{7}$$

where coefficient A_3 is expressed through A_2 and G. In (7) we introduced coefficient

$$\alpha_{qs} = \frac{A_1}{A_3} \tag{8}$$

which is a weak function of temperature T and pressure P. Similar to (3) formulation (7) demonstrates that CR is a linear function of upward mass flux. By comparing the LES derived formulation (3) with the theoretical formulation (7), one can obtain κ as:

$$\kappa = \alpha_{les}/\alpha_{qs} \tag{9}$$

In order to evaluate α_{qs} which is a function of temperature T and pressure P, we first calculate at each vertical level the values of T and P as horizontal averages over the cloudy areas, and then obtain α_{qs} using (8), and expressions for A_1 and A_3 which are functions of temperature T and pressure P. The values of α_{les} are calculated as slopes of linear fits either to the full LES dataset ($\alpha_{qs} = 2.06$), or to each individual group subset (2.17, 2.13, 2.052, and 2.049 for G1-G4 groups, respectively, see Fig. 2).

The vertical profile of κ is shown in Fig. 3 for two times in cloud system evolution. The top panel refers to an early cloud system formation (t = 8 hrs) when only small clouds in G1/G2

groups were formed. The bottom panel refers to t = 24 hrs when the cloud system has already been fully developed with clouds present in all groups.

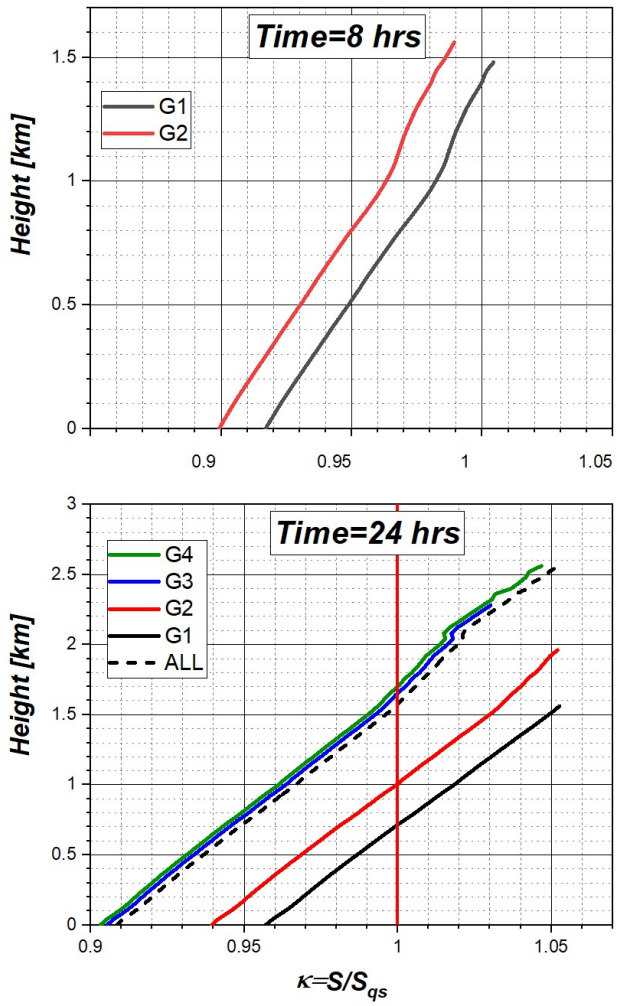

Figure 3. Vertical profile of the ratio of supersaturation to its quasi=steady value. Top panel- the early stage of cloud formation (time=8 hrs), bottom panel – the mature stage of cloud system development (time=24 hrs). The vertical coordinate denotes the height above the cloud base.

As Fig. 3 shows, in the early formed clouds at t= 8 hrs the supersaturation is, on average, smaller by 3-5% than its quasi-steady value (top panel). This is the result of small values of integral radius R_i at the early stage of cloud formation, which combined with growing updrafts leads to large quasi-steady supersaturations (eq. 5). At the mature stage R_i is larger, resulting in

the decrease of S_{qs}. The decrease in S_{qs} is especially pronounced below cloud tops where updrafts approaching the inversion layer are weak. The cloud supersaturation S, on the other hand, may increase there because of the entrainment and mixing with cold environmental air. While all these factors may qualitatively explain the increase of κ with height, the more accurate profile of κ may be obtained by accounting for vertical variation of α_{les}. The profiles shown in Fig. 3 consider only constant with height integral values of α_{les}; i.e., averaged over the whole cloud.

Contrasting observational and theoretical relationships (3) and (7) may provide a method for estimating supersaturation in clouds. As it is well known, the direct measurements of S are quite difficult; using instead concurrent measurements of vertical velocities and temperatures for calculating condensation rates, will allow to obtain observational values of α_{obs} similar to (1), with observational data replacing LES datasets. The value of κ then can be obtained from (9) where α_{les} is replaced by α_{obs} , and, finally, supersaturation S can be calculated according to (6).

MAJOR FINDING

1. Data from LES simulations of shallow cumulus clouds demonstrates a nearly perfect correlation between condensation rate (CR) and upward (positive) mass flux (MFP). This strong correlation is explained using the condensation theory. The strong CR-MFP correlation implies that supersaturation in clouds varies within a few percent of its quasi-steady value.

2. Calculating the slope of the CR-MFP linear fit from concurrent measurements of temperature and vertical velocity, and comparing it with the corresponding slope based on the quasi-steady supersaturation assumption, may provide a method for estimation of supersaturation in clouds.

3. The strong dependence of condensation rates on vertical velocity may indicate the direction for development of SGS latent heat release parameterization.

REFERENCES

Cooper, W. A., 1989: Effects of variable droplet growth histories on droplet size distributions. Part I: Theory. *J. Atmos. Sci.,* 46, 1301–1311, doi:10.1175/1520-0469(1989)046,1301: EOVDGH.2.0.CO;2.

Khairoutdinov, M. F., and D. A. Randall, 2003: Cloud resolving modeling of the ARM summer 1997 IOP: Model formulation, results, uncertainties, and sensitivities. *J. Atmos. Sci.*, **60**, 607–625.

Kogan Y. L., 2013: A Cumulus Cloud Microphysics Parameterization for Cloud-Resolving Models. *J. Atmos. Sci.,* **70**, 1423-1436.

Kogan, Y. L., 2021: LES study of precipitation/condensation dependence on cumulus clouds dynamics, Adv. Sci. Res., 18, 89–92, https://doi.org/10.5194/asr-18-89-2021.

Korolev, A., and I. P. Mazin, 2003: Supersaturation of water vapor in clouds. J. Atmos. Sci., 60, 2957–2974, doi:10.1175/ 1520-0469(2003)060,2957:SOWVIC.2.0.CO;2.

Paluch, I. R., and Ch. A. Knight, 1984: Mixing and evolution ofcloud droplet size spectra in vigorous continental cumulus.J. Atmos. Sci., 41, 1801–1815.

Pinsky, M., I. P. Mazin, A. V. Korolev, and A. Khain, 2013: Supersaturation and diffusional droplet growth in liquid clouds. J. Atmos. Sci., 70, 2778–2793, doi:10.1175/JAS-D-12-077.1.

Politovich, M. K., and W. A. Cooper, 1988: Variability of the supersaturation in cumulus clouds. *J. Atmos. Sci*., 45, 1651–1664, doi:10.1175/1520-0469(1988)045,1651:VOTSIC.2.0.CO;2.

Siebert, H., and R. A. Shaw, 2017: Supersaturation Fluctuations during the Early Stage of Cumulus Formation., *J. Atmos. Sci.,* 74, 975-988. DOI: 10.1175/JAS-D-16-0115.1

Squires, P., 1952: The growth of cloud drops by condensation. Aust.J. Sci. Res., 5, 59–86.

vanZanten, M. C., and 19 co-authors, 2011: Controls on precipitation and cloudiness in simulations of trade-wind cumulus as bserved during RICO. *J. Adv. Model. Earth Syst.*, 3, M06001, doi:10.3894/JAMES.2011.3.5